Methyl and carbon–carbon double bond in anhydride molecules modulated surface charge trap depth of epoxy materials

Yushun Zhao, Yufan Xu, Gilbert Teyssèdre, Jianyi Xue, Yanning Zhao, Bin Du

Methyl and carbon-carbon double bond in anhydride molecules modulated surface charge trap depth of epoxy materials

Yushun Zhao[1], Yufan Xu[1], Gilbert Teyssèdre[2], Jianyi Xue[1], Yanning Zhao[1] and Bin Du[1]

Electrical Engineering Department, Hefei University of Technology, Hefei, Anhui, 230009 China
[2] LAPLACE (Laboratoire Plasma et Conversion d'Energie), University of Toulouse, 118 route de Narbonne, F-31062 Toulouse Cedex 9, France

Abstract—Epoxy insulators in gas insulated switchgear and gas insulated transmission lines tend to accumulate surface charges, leading to insulation flashover. Improving the surface trap characteristics of epoxy materials, which can accelerate the surface charge dissipation of epoxy insulators, is a promising method to improve the surface insulation performance. The surface trap characteristics of epoxy materials are strongly influenced by the chemical groups in the acid anhydride molecules. In this work, by quantum chemical calculations and isothermal surface potential decay tests, taking six organic anhydrides that differ only in the methyl and carbon–carbon double bonds, we find the modulation laws of methyl and carbon–carbon double bonds on the charge trap depth within and between molecular chains. The regulation mechanism is revealed from the microscopic perspectives of electron energy structure and electron cloud offset. The changes of surface charge trap depth of epoxy materials are primarily attributed to the changes in the spatial distribution of the electron cloud density between and on the valence bonds caused by the interaction between the electron-donating methyl group and the electron-absorbing carbon–carbon double bond.

Index Terms—Epoxy resin, acid anhydride, chemical group, quantum chemical calculation, trap depth

1. Introduction

As a polymer dielectric with excellent electrical properties, epoxy resin is widely used in gas-insulated switchgear (GIS) and gas-insulated transmission lines (GIL) [1, 2]. However, after long-term operation under DC voltage, the surface of epoxy materials tends to accumulate a large amount of charge, leading to distorted electric field distribution and insulation flashover. Improving the surface charge trap characteristics of epoxy materials can accelerate the surface charge dissipation and suppress the surface electric field distortion, thus improving the DC insulation performance [3-5]. It has been shown that the surface charge trap characteristics of polymer dielectrics are strongly affected by the chemical groups in the polymer molecular chains [6-10]. The chemical groups introduce local state traps into the band gap of polymer dielectrics, which affect the trap depth and DC insulation performance of polymer dielectrics. The trap characteristics in insulating polymers in previous investigations determined by quantum chemical calculations were concerned with chemical defects in polyethylene [11]. Over the years, the calculation method was refined by considering different types of chemical defects and crosslinking residues nanocomposites [12, 13]. The prediction issued from molecular simulations were compared with experimental results, for example the kinetics of positive charge propagation in polyethylene [14]. Interesting aspects also concern the change in electronic properties due to ageing: density functional theory (DFT) calculations were used to compare the trap energies of charge traps produced by chemical groups, including the produced carbon–carbon double bonds, conjugated double bonds, and carbonyl groups during thermal degradation [15]. Afterwards, the technique was applied to design the insulating polymers. For example, quantum chemical calculations coupled to isothermal surface potential decay (ISPD) were used to design the epoxy resin molecules with investigating the effect of grafting trifluoromethyl (–CF3) groups. The results showed that –CF3 introduced electron traps in the epoxy material, thus hindering the dissipation of electrons on the surface of the epoxy material [16].

Organic anhydrides can form cross-linked networks with epoxy resins which have excellent dielectric and insulating properties, making them the most commonly used curing agents in the preparation of epoxy materials [17, 18]. Among them, hexahydrophthalic anhydride (HHPA), tetrahydrophthalic anhydride (THPA), phthalic anhydride (PA), methyl hexahydrophthalic anhydride (Me-HHPA), methyl tetrahydrophthalic anhydride (Me-THPA), and methyl nadic anhydride (MNA) are the six most common organic anhydride curing agents available in the market. These anhydride curing agents only differ in the chemical groups of methyl and carbon–carbon double bonds. Therefore, it can be easily concluded that the chemical groups methyl and carbon– carbon double bonds in anhydride molecules will modulate the chemical structure of epoxy resin/anhydride cross-linked molecules, and potentially the surface charge trap depth of the epoxy materials.

In this paper, by comparing the distributed energy levels of above six geometrically optimized epoxy resin/anhydride cross-linked molecules, we found the modulation laws of

methyl and carbon–carbon double bonds on the intramolecular charge trap depth in epoxy materials. In addition, by analyzing the ISPD test data, we found the modulation laws of methyl and carbon–carbon double bonds on the intermolecular charge trap depth in epoxy materials. This paper focuses on explaining these regulation laws from the microscopic perspectives of electron energy structure and electron cloud offset, in order to provide theoretical references for the structural design and surface charge trap modulation of polymer materials.

2. Quantum Chemical Calculations

2.1. Six epoxy resin/anhydride molecules

Epoxy polymer dielectrics are usually obtained from the cross-linking curing process of epoxy resins and curing agents. Here, taking bisphenol-A type epoxy resin (DGEBA) as an example, we considered the minimum periodic structure of the cross-linked network. It was formed by cross-linking of one DGEBA molecule and two acid anhydride molecules, as shown in Fig. 1a, called DGEBA/AH molecule. In Fig. 1a, R_n is the anhydride molecule after opening the five-membered ring.

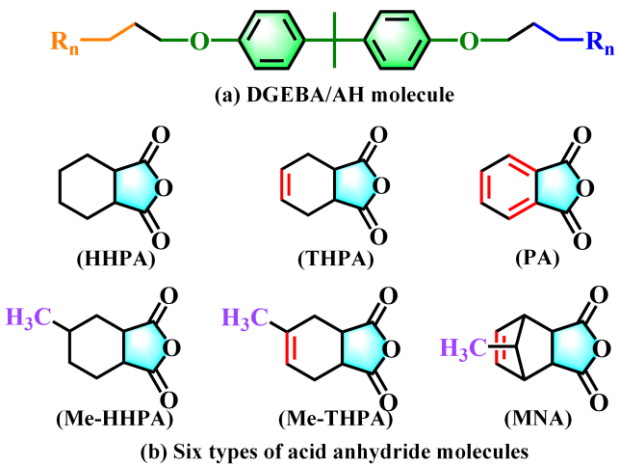

Fig. 1. Molecular structure diagrams.

Fig. 1b shows the molecular structures of six common anhydride curing agents, which are HHPA, THPA, PA, Me-HHPA, Me-THPA and MNA. In contrast to HHPA molecule, the Me-HHPA molecule has a methyl group introduced at the meta-position of the anhydride group. Compared to THPA molecule, the Me-THPA molecule introduces a methyl group at the meta-position of the anhydride group. In contrast to THPA molecule, the MNA molecule introduces a methyl group by being attached to a bridge ring. Compared to HHPA molecule, the THPA molecule has a carbon-carbon double bond at the para-position of the anhydride group. In contrast to Me-HHPA molecule, the Me-THPA molecule has a carbon-carbon double bond at the para-position of the anhydride group. Compared to HHPA molecule, the PA molecule introduces a carbon-carbon double bond at both the para and adjacent positions of the anhydride group.

The methyl and carbon-carbon double bond in anhydride molecule are an electron-donating group and an electron-absorbing group, respectively. After they are introduced into a certain molecular segment, the electron interaction between them changes the electron cloud density between and on valence bonds in the segment, which may cause the change of the lowest unoccupied molecular orbital (LUMO) energy level and the highest occupied molecular orbital (HOMO) energy level of the segment. In other words, the change magnitude in the LUMO and HOMO energy levels of the segment may be related to the interaction intensity between the electron-donating group methyl and the electron-absorbing group carbon-carbon double bond. The changes in the LUMO and HOMO energy levels of adjacent segments determine the changes in the charge trap depth within the molecular chain [19]. The quantification of energy level changes is obtained using quantum chemical calculations, as shown in the following section.

2.2. Charge trap depth of the DGEBA/AH molecule

Below we analyzed the effect of methyl and carbon–carbon double bond on the charge trap depths based on ideal molecular groups, ignoring factors such as pending bonds and defects. The geometries of each oligomer were optimized by DFT using Gaussian 09 software, and their energy level distribution and molecular orbital information were obtained. The B3LYP hybrid functional method and 6–31 G(d) basis function set, widely adopted to simulate low molecular weight polymers, were used in the calculations.

Fig. 2 shows the energy band structure and distributed energy levels of DGEBA/THPA molecule. The zero level in the band diagram is the vacuum energy level. Fig. 2(b) shows the energy band structure of the DGEBA/THPA molecule. In Fig. 2(b), if we focus on the molecular orbital corresponding to an energy level, the molecular orbital is locally distributed along the molecular chain. Therefore, we can obtain the distributed energy levels of DGEBA/THPA molecules on different segments. The DGEBA/THPA molecule is divided into two anhydride segments and one resin segment, and its distributed energy level values and numbers are shown in Fig. 2(c). In three dimensions, the spatial arrangement of the same type of atoms in segments A and C is not perfectly symmetrical, therefore, the energy levels of segments A and C are different.

Comparing Fig. 2b and Fig. 2c, it can be seen that the LUMO energy level of segment C is the LUMO energy level of the whole DGEBA/THPA molecule, and the HOMO energy level of segment B is the HOMO energy level of the whole DGEBA/THPA molecule. The molecular orbital distribution corresponding to the LUMO and HOMO energy levels of the DGEBA/THPA molecule are shown in Fig. 2c. If extra electrons captured at the LUMO of a molecular segment drift toward its neighboring segment under an electric field, the captured electrons need to overcome an energy barrier, which means that the LUMO of the segment is an electron trap site, and the energy barrier height is the depth of the electron trap created by that site [14]. Similarly, if extra holes captured at the HOMO of a molecular segment drifts toward its neighboring segment under an electric field, the captured holes need to overcome an energy barrier, which means that the HOMO of

the segment is a hole trap site, and the energy barrier height is the depth of the hole trap created by that site.

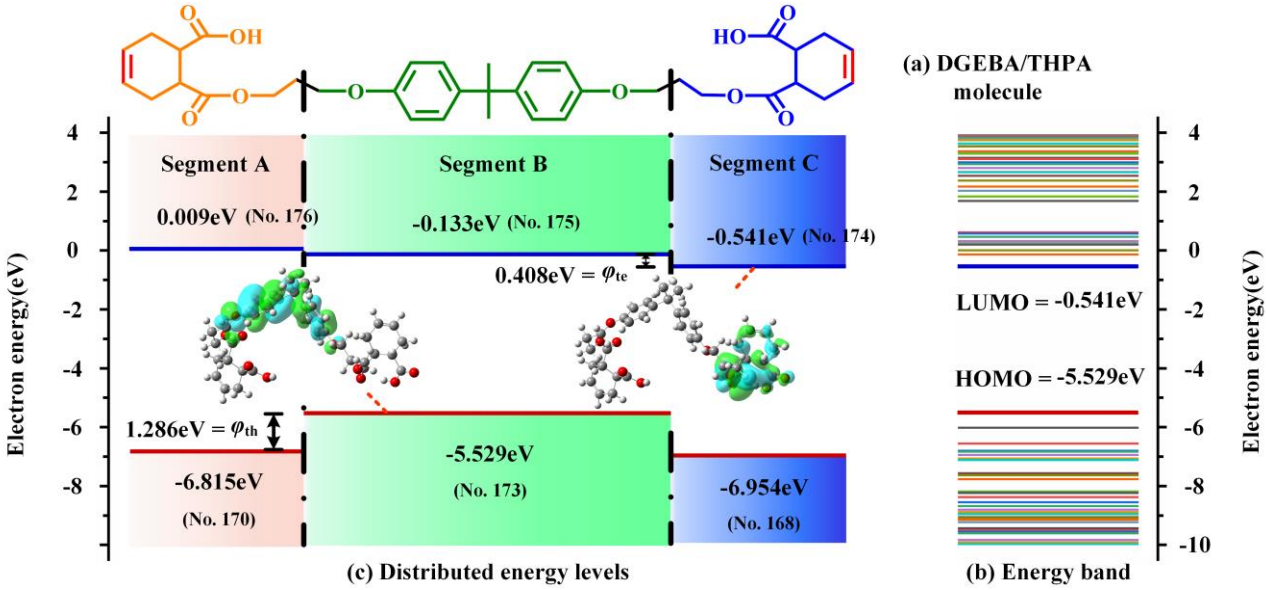

Fig. 2. The energy band structure and distributed energy levels of DGEBA/THPA molecule

.

As shown in Fig. 2c, the LUMO energy level of segment C is an electron trap site, which produces an electron trap depth φ_{te} of 0.408 eV; the HOMO energy level of segment B is a hole trap site, which produces a hole trap depth φ_{th} of 1.286 eV.

Following the same division of the segments as above, we obtained the charge trap depths for the other five DGEBA/AH molecules. The charge trap depths of all DGEBA/AH molecules are listed in Table. I.

TABLE I CALCULATED CHARGE TRAP DEPTH PARAMETERS

Molecule types	φ_{te} (eV)	φ_{th} (eV)
DGEBA/HHPA	0.460	1.286
DGEBA/THPA	0.408	1.286
DGEBA/PA	1.804	1.749
DGEBA/Me-HHPA	0.464	1.280
DGEBA/Me-THPA	0.402	1.034
DGEBA/MNA	0.159	0.937

2.3. Modulation of charge trap depths within molecules by methyl

As shown in Table I, the electron and hole trap depths of DGEBA/Me-HHPA molecule are almost unchanged, compared with that of DGEBA/HHPA molecule; the electron and hole trap depths of DGEBA/MNA molecule are both slightly decreased, compared with those of DGEBA/THPA molecule. It can be found that when there is no carbon–carbon double bond in the original anhydride molecule, the introduction of methyl has almost no effect on the charge trap depths of DGEBA/AH molecule; when there is a carbon–carbon double bond in the original anhydride molecule, the introduction of methyl causes the charge trap depths of DGEBA/AH molecule to show a decreasing trend, which may be related to the interaction between the methyl and carbon–carbon double bond. A detailed discussion is described below.

Fig. 3 shows the energy band structure and distributed energy levels of DGEBA/Me-THPA molecule. The variation of the charge trap depths within molecules is determined by the variation of the distributed energy levels. Comparing Fig. 2c and Fig. 3c, it can be seen that the distributed energy levels of DGEBA/Me-THPA molecule do not change significantly compared to those of DGEBA/THPA molecule, except for a small increase in the HOMO energy level of segment A and the HOMO energy level of segment C. We tried to explain these variations.

If an electron-absorbing group is introduced into a molecular segment, due to electrostatic interactions, the group will attract the orbital electrons between and on the valence bonds in the segment. When the orbital electrons between the valence bonds are attracted by the group, the orbital electrons shift towards the positively charged center of the group, and the electron cloud density between the positively charged center and the atom whose orbital electrons have shifted increases. This makes the electron orbital system between the valence bonds in the segment more stable, so the energy of the orbital electrons (conduction band electrons) moving between the valence bonds decreases, the LUMO energy level of the segment decreases [20]. When the orbital electrons on the valence bonds are attracted by the electron-absorbing group, the orbital electrons shift towards the positively charged center of the group. In this way, the electron cloud density on the valence bonds decreases, and the overlap of the electron cloud is reduced. This makes the covalent bonds formed between the bonding atoms more unstable, so the energy of the orbital electrons (valence band electrons) moving on the valence bonds increases, the HOMO energy level of the segment increases [20].

In the anhydride segment of the DGEBA/THPA molecule, there is an electron-absorbing group carbon-carbon double

bond. In contrast to that of DGEBA/THPA molecule, one of the carbon atoms of carbon-carbon double bond in DGEBA/Me-THPA molecule connects an electron-donating group methyl through a covalent bond. The carbon-carbon double bond attracts orbital electrons on the covalent bonds connected to the carbon atom in the methyl, resulting in a decrease in the electron cloud density on the valence bonds. From the above analysis, the HOMO energy levels of the anhydride segments will be elevated. The spatial configuration of the three atoms connected to the carbon atom of the carbon-carbon double bond is planar triangular type, which makes a long spatial distance between the carbon-carbon double bond and the orbital electrons between the valence bonds provided by methyl, and their electrostatic attraction is weak. There is no obvious change in the electron cloud density between the original valence bonds, therefore, the introduction of methyl does not cause any significant variation in the LUMO energy levels of the anhydride segments.

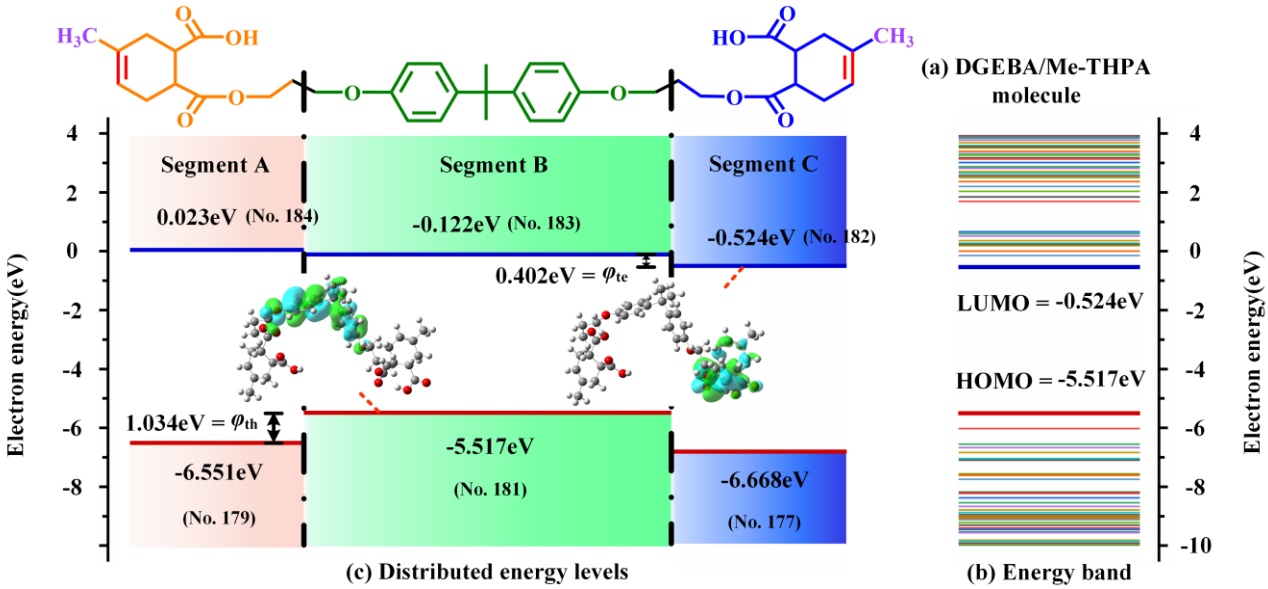

Fig. 3. The energy band structure and distributed energy levels of DGEBA/Me-THPA molecule.

Similarly, the introduction of methyl leads to an increase in the HOMO energy level of the anhydride segment, therefore, the hole trap depth of DGEBA/MNA molecule also shows a small decrease. Differently, the methyl in DGEBA/MNA molecule is attached to a bridge ring, which is easily attracted to the carbon-carbon double bond and moves to a position near it in the three-dimensional space. In this way, the attraction of the carbon-carbon double bond to the orbital electrons between the original valence bonds is weakened, and the electron cloud density between the original valence bonds is reduced. This causes an increase in LUMO energy level of the anhydride segment, so the electron trap depth of the DGEBA/MNA molecule shows a small decrease.

2.4. Modulation of charge trap depths within molecules by carbon-carbon double bond

Compared with that of DGEBA/Me-HHPA molecule, the electron trap depth of DGEBA/Me-THPA molecule decreases slightly, and the hole trap depth shows a small reduction; compared with that of DGEBA/HHPA molecule, the electron trap depth of DGEBA/THPA molecule decreases slightly, while the hole trap depth does not change; compared with that of DGEBA/HHPA molecule, the electron trap depth of DGEBA/PA molecule increases substantially, and the hole trap depth increases slightly. The changes in charge trap depth of distributed energy levels are compared.

Fig. 4 shows the energy band structure and distributed energy levels of DGEBA/Me-HHPA molecule. In contrast to those of DGEBA/Me-HHPA molecule, the LUMO energy level of anhydride segment of DGEBA/Me-THPA molecule tends to increase slightly, and the HOMO energy level of anhydride segment shows a small increase; the LUMO energy level of resin segment of DGEBA/Me-THPA molecule does not change, while the HOMO energy level of resin segment shows a small increase.

The carbon atoms in carbon-carbon single bonds are sp^3 hybridized, and carbon atoms in carbon-carbon double bonds are sp^2 hybridized. The s-orbital electrons move close to the nucleus and have a weak shielding effect on the nucleus. Therefore, the larger the s-orbital component contained in the hybridized orbital of a bonding atom, the stronger the attraction of the bonding atom to its surrounding electrons. This makes the attraction of the carbon atoms to its surrounding electrons stronger when the carbon-carbon single bond changes to a carbon-carbon double bond.

In the anhydride segment of DGEBA/Me-HHPA molecule, there is an electron-absorbing group ester group, as shown in Fig. 4a. The ester group attracts the orbital electrons between the valence bonds in anhydride segment, which increases the electron cloud density near the positively charged center of it. After the introduction of the para carbon-carbon double bond, as shown in Fig. 3a, it will have a slight attraction to the orbital electrons. This causes the average motion radius of the orbital

electrons to increase and the electron cloud density near the positively charged center to decrease. Therefore, the LUMO energy level of the anhydride segment of DGEBA/Me-THPA molecule tends to be slightly elevated. In addition, the introduced carbon-carbon double bond is directly connected to the methyl through a covalent bond. The carbon-carbon double bond attracts the orbital electrons on valence bonds in the anhydride segment, which makes the electron cloud density on valence bonds show a small decrease. As a result, the HOMO energy level of anhydride segment of the DGEBA/Me-THPA molecule shows a small elevation.

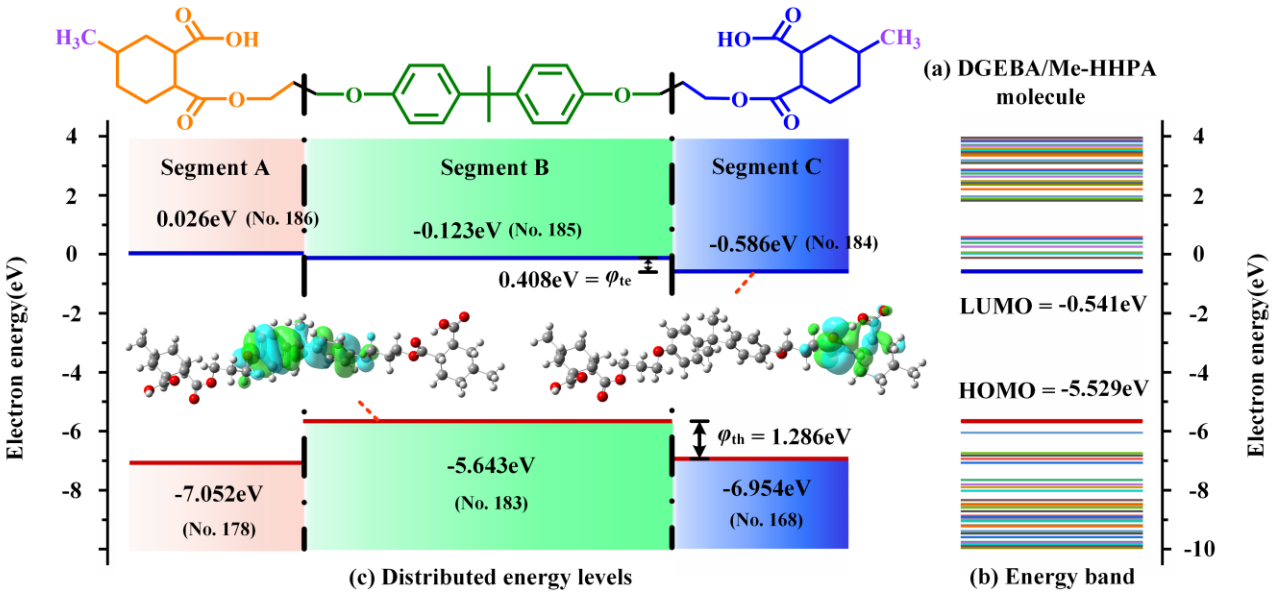

Fig. 4. The energy band structure and distributed energy levels of DGEBA/Me-HHPA molecule.

In the resin segment of DGEBA/Me-HHPA molecule, the 2p orbital of the oxygen atom in the ether oxygen group connected with the benzene ring forms a p-π conjugation with the large π orbitals of the benzene rings, which makes the electron cloud density between the conjugated atoms lower and the internal energy of the conjugated system lower, thus forming a more stable conjugated system [20]. In contrast to those of the DGEBA/Me-HHPA molecule, the anhydride segments of the DGEBA/Me-THPA molecule are curled toward the resin segment in three-dimensional space, as can be seen in Fig. 3c. Under the electrostatic effect of the electron-absorbing group ester group in anhydride segment, the conjugation degree between the p-orbital and the large π-orbital in resin segment is reduced, which makes the p-π conjugated system more unstable. As a result, the HOMO energy level of resin segment of the DGEBA/Me-THPA molecule shows a small increase.

After the introduction of carbon-carbon double bond, the variation trends of distributed energy levels of DGEBA/THPA molecule are consistent with those of the DGEBA/Me-THPA molecule, which will not be discussed here.

In the anhydride segment of the DGEBA/PA molecule, the 2p orbitals of the carbon atoms in the three carbon-carbon double bonds introduced are parallel to each other and overlap, forming a highly delocalized large π orbital perpendicular to the benzene ring plane. The delocalized large π orbital electrons between the valence bonds in anhydride segment are readily attracted to the ester group, which results in a substantial increase in the electron cloud density near the positively charged center of the ester group. Therefore, compared to those of the DGEBA/HHPA molecule, the LUMO energy level of anhydride segment of the DGEBA/PA molecule is substantially lower and the electron trap depth of the DGEBA/m molecule is significantly increased. The ester group in the curled anhydride segment makes the p-π conjugated system in the resin segment more unstable, as described earlier. This leads to a small increase in the HOMO energy level of the resin segment and a small increase in the hole trap depth of the DGEBA/PA molecule.

In the above we analyzed the modulation laws on charge trap depth within the molecular chains. However, in general, the excess electrons would be localized at the AH ends, then, it is what happens at chain end that controls the actual transport. In other words, the interchain charge transport influenced by the chain-end groups controls the actual charge transport. Different chain-end groups produced different interchain charge transport situations, which may lead to different ISPD results. The following sections analyze the modulation of electron trap depth between molecular chains through ISPD experimental results.

3. Isothermal Surface Potential Decay Tests

3.1. Experimental raw materials

The bisphenol-A type epoxy resin is branded as DER331. It is chemically pure, with an epoxy value of 0.535 mol/100g, purchased from Shanghai Kaiyin Chemical Co., Ltd. Anhydride curing agent: HHPA, chemically pure; THPA, chemically pure; Me-HHPA, chemically pure; Me-THPA, chemically pure;

MNA, chemically pure. These anhydride curing agents were purchased from Shanghai Macklin Biochemical Co., Ltd, and their molecular structures were shown in Fig. 1. Curing accelerator: N, N-dimethylbenzylamine (BDMA), purchased from Shanghai Aladdin Biochemical Technology Co., Ltd.

3.2. Sample preparation

Equation (1) is the formula for calculating the anhydride mass per 100 g of epoxy resin, in where W_h is the relative molecular weight of the anhydride, E_v is the epoxy value of the epoxy resin, k is the correction coefficient.

$$\text{Anhydride dosage} = W_h * E_v * k \quad (1)$$

Table II shows the curing formulations of six DGEBA/AH systems. The mass of BDMA added was 0.6% (0.6 g) of the mass of epoxy resin in the curing systems. The resin and curing agents were weighed and poured into the reaction kettle in turn. They were evenly dispersed with a high-speed disperser at a constant temperature of 353.15 K, and a vacuum degassing treatment was performed simultaneously. After mixing thoroughly, the BDMA was added to the reaction kettle and the high-speed dispersion and vacuum degassing treatment were continued. Afterwards, the resin castings were poured into the mold (the mold should be preheated in a constant temperature oven at 353.15 K for at least 3 h before casting). After putting the mold into a constant temperature oven, the oven was vacuumed for 6 min. The resin castings were cured at 353.15 K for 4 h and at 393.15 K for 12 h to obtain the cured epoxy samples. The cured samples are circular-shaped with a diameter of 100 mm and a thickness of 1 mm. Before the ISPD tests, all samples were cleaned by anhydrous alcohol and deionized water in an ultrasonic cleaner, and then dried in a baking oven at 333.15 K for 24 h, in order to eliminate the humidity and the residual charges inside the materials.

TABLE II FORMULATIONS OF DGEBA/AH SYSTEMS

Anhydride type	Relative molecular mass	AH/g	DGEBA/g
HHPA	154.16	1.286	100
THPA	152.15	1.286	100
PA	148.12	1.749	100
Me-HHPA	168.19	1.280	100
Me-THPA	166.18	1.034	100
MNA	178.18	0.937	100

The cured samples are circular-shaped with a diameter of 100 mm and a thickness of 1 mm. Before the ISPD tests, all samples were cleaned with anhydrous alcohol and deionized water in an ultrasonic cleaner, and then dried in a baking oven at 333.15K for 24 h, in order to eliminate the humidity and the residual charges inside the materials.

3.3. ISPD measurement

The ISPD was tested with a needle-mesh grid-plate electrode system. Fig. 5 shows the schematic diagram of the experimental setup. The needle electrode is 2 cm from the mesh grid electrode, and the mesh grid electrode is 1 cm from the grounded electrode. During the test, the needle electrode and mesh grid electrode are applied with -10 kV and -6kV DC high voltage, respectively.

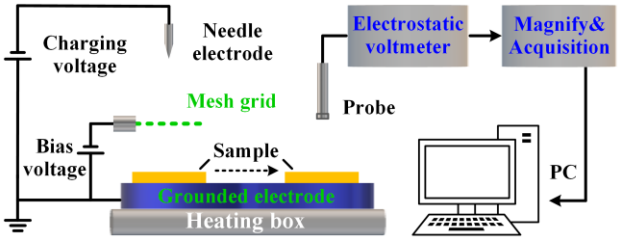

Fig. 5. Experimental setup for ISPD measurement.

After charged for 10 min, the samples are moved to the Kelvin probe of electrostatic voltmeter in 1 s via a rotatable platform. The distance between the probe and the sample surface is kept as 2 mm. The samples with smooth surface are selected for good contact with the grounded electrode. All experiments are carried out in an airtight chamber with the measurement temperature keeping constant as 323.15 K.

4. TEST RESULTS AND DISCUSSIONS

4.1. Surface potential decay results

Fig. 6 shows the normalized ISPD curves of DGEBA/AH cured samples after negatively corona charging at the temperature of 323.15 K. These curves were obtained by fitting the ISPD data with a double exponential decay equation. The double exponential decay equation represents the simultaneous occurrence of charge decay processes controlled by shallow and deep traps, so the normalized potential can directly reflect the characteristics of the potential decay [19].

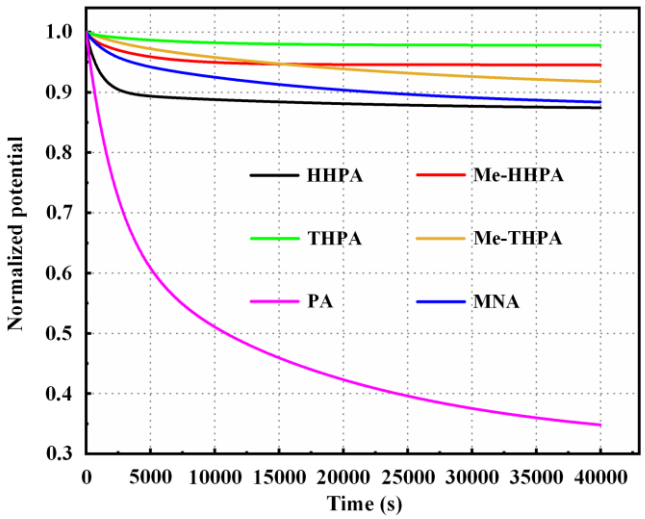

Fig. 6. Normalized surface potential decay of the DGEBA/AH cured samples.

As can be seen in Fig. 6, the normalized surface potentials of the DGEBA/PA and DGEBA/HHPA samples decay much faster in the early stages than in the later stages. This indicates that there are more shallow electron traps in the DGEBA/PA and DGEBA/HHPA samples. More deep electron traps are

present in the other four DGEBA/AH samples. In addition, after a long decay time, the normalized surface potentials of the samples are still high except for the DGEBA/PA sample, indicating that substantial deep trapped electrons need a longer time and a higher temperature to be excited.

4.2. Surface trap energy distribution results

The relationship between the surface trap depth (E_t) and the surface trap density (N_t) are shown in (2) and (3), where k is the Boltzmann constant, T is the absolute temperature, v is the attempt-to escape frequency of trapped electron, $4.17\times10^{13}s^{-1}$, t is the decay time, ε_0 is the vacuum dielectric constant, ε_r is the relative dielectric constant, q_e is the electron charge, L is the sample thickness, V is the surface potential [19].

$$E_t = kT\ln(v\cdot t) \tag{2}$$

$$N_t = \frac{\varepsilon_0\cdot\varepsilon_r}{q_e\cdot L}\cdot t\frac{dV}{dt} \tag{3}$$

According to (2) and (3), the surface trap distribution of the six DGEBA/AH cured samples can be obtained, as shown in Fig. 7. DGEBA/PA and DGEBA/HHPA samples have higher peak densities of shallow electron traps than deep electron traps. The other four DGEBA/AH samples are the opposite. These are consistent with the results obtained from the normalized surface potential decay curves. It is worth noting that DGEBA/Me-HHPA, DGEBA/THPA, and DGEBA/Me-THPA samples do not show a significant shallow trap density peak.

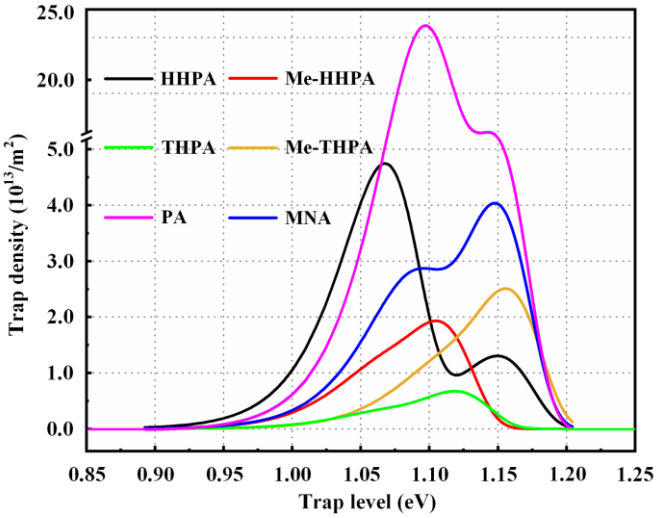

Fig. 7. Surface Trap Energy Distribution of the DGEBA/AH cured samples.

The differences in the distribution of shallow and deep traps indicate the structural differences in the polymer materials. The effect of methyl and carbon–carbon double bond on the aggregation structure between the molecular chains may have led to the structural differences. The wave function of the conduction band edge has inter-chain characteristics. The conduction electrons in the lowest energy state are naturally channeled out of the dense regions, and they tend to move to the low-density regions. As a result, the extra electrons tend to move into the low-density regions where many electron traps are formed. In DGEBA/AH crosslinked molecules, the methyl and the carbon–carbon double bond contributed by the anhydride molecule are located at the chain ends. Due to the electrostatic attraction, the methyl and the carbon–carbon double bond at the chain ends will lead to a more condensed interchain distance and less free volume. The extra electrons are localized in small free volume spaces and have difficulty moving freely, which makes the small free volume spaces behave as deep electron traps. THPA, Me- HHPA, Me-THPA, and MNA molecules all contain methyl or carbon–carbon double bond, so the resin samples cured by these anhydrides contain more inter-chain deep electron traps. In addition, the chain-terminal carbon–carbon double bond provides a stronger attraction between the extra electrons and the surrounding macromolecular chains. This attraction will further localize the electrons and deepen the inter-chain electron trap depth. Therefore, the resin samples cured by THPA, Me-THPA, and MNA have deeper inter-chain electron traps, as shown in Fig. 7.

The HHPA molecule has neither methyl nor carbon-carbon double bond. Therefore, the samples cured by HHPA have expanded inter-chain distances and larger free volume spaces, forming shallower electron traps. This is consistent with the results in Fig. 7.

Compared to the HHPA-cured samples, the PA-cured samples have a higher density of shallow and deep electron traps. This is due to a highly delocalized large π orbital in the benzene ring of the PA molecule. On the one hand, the large π orbital electrons of the chain-terminal benzene ring of adjacent DGEBA/PA molecules strongly repel each other, resulting in a large free volume space in the chain end regions, where form a high density of shallow electron traps. On the other hand, the strong repulsive effect causes the obvious internal bending and folding of the molecular chains, leading to a small free volume space in the internal folding regions, where form a high density of deep electron traps. Both the depth and density of the traps affect the charge transport. The shallower traps allow charges to transport in hopping through multiple detrapping and trapping steps, which facilitates charge transport. The higher trap density reflects the smaller trap distance, which may lead to the overlap of trap wave-functions. This allows charges to tunnel from one localized state to another without transition to extended state, facilitating the charge transport. The surface potential decay in the early stage is related to the electron transport in the shallow traps. Although the electron trap of PA-cured sample is not the shallowest, its shallow electron trap density is much higher than that of other samples. This facilitates the tunneling transport of electrons, resulting in the fastest initial decay rate.

Conclusion

This study investigates the modulation mechanism of surface charge trap depth in epoxy materials by methyl and carbon–carbon double bonds in anhydride molecules, based on quantum chemical calculations and ISPD tests. The conclusions are summarized as follows:

(1) When there is no carbon–carbon double bond in the original anhydride molecule, the introduction of methyl has almost no effect on the charge trap depths of the DGEBA/AH molecule. When there is a carbon–carbon double bond in the original anhydride molecule, the introduction of methyl causes the charge trap depths of the DGEBA/AH molecule to show a decreasing trend.

(2) The introduction of one carbon–carbon double bond results in a slight decrease in the charge trap depth of the DGEBA/AH molecule, while the introduction of three carbon–carbon double bonds results in a significant increase in that. The interaction between the methyl group and carbon–carbon double bond changed the spatial distribution of the electron cloud density between and on the valence bonds, which subsequently changed the charge trap depth of the DGEBA/AH molecule.

(3) The PA-cured samples have a much higher density of shallow electron traps than that of other samples. This facilitates the tunneling transport of electrons, leading to the fastest initial decay rate.

References

[1] Ruan H, Xie Q, Yan J, Song J, Zhan Z and Lü F 2021 Enhanced DC surface insulation of Al2O3/ER brought by the permeability of fluorine-containing release agent *IEEE Trans. Dielectr. Electr. Insul.* **28** 762–70

[2] Shimakawa H, Kumada A, Hidaka K, Sato M, Yasuoka T, Hoshina Y and Shiiki M 2021 One-dimensional modeling of charge transport in epoxy for DC-GIS insulating spacer *IEEE Trans. Dielectr. Electr. Insul.* **28** 1457–64

[3] Wang F, Liang F, Chen S, Zhong L, Sun Q, Zhang B and Xiao P 2021 Effect of surface charges on flashover voltage-an examination considering charge decay rates *IEEE Trans. Dielectr. Electr. Insul.* **28** 1053–60

[4] Yadam Y R, Guvvala N, Arunachalam K and Ramanujam S 2022 Understanding charge trap characteristics of epoxy nanocomposite under steep fronted lightning impulse voltage *Electr. Eng.* **104** 567–76

[5] Du B and Li A 2017 Effects of DC and pulse voltage combination on surface charge dynamic behaviors of epoxy resin *IEEE Trans. Dielectr. Electr. Insul.* **24** 2025–33

[6] Li J, Wang Y, Ran Z, Yao H, Du B and Takada T 2020 Molecular structure modulated trap distribution and carrier migration in fluorinated epoxy resin *Molecules* **25** 3071

[7] Akram S, Zhou K, Meng P, Castellon J, Agnel S, Wang P, Nazir M T, Chen Y and Hussain H 2021 Charge transport and trapping of surface modified stator coil insulation of motors *IEEE Trans. Dielectr. Electr. Insul.* **28** 719–26

[8] El-Shahat M, Huzayyin A and Anis H 2019 Effect of chemical impurities on charge injection barriers at the interface of copper and polyethylene *IEEE Trans. Dielectr. Electr. Insul.* **26** 642–7

[9] Mai Y, Du B, Zhao Y, Liu Q and Yang W 2022 Modulation of epoxy polymer trapping energy levels by fluorinated diluents to improve insulation properties *IEEE Trans. Dielectr. Electr. Insul.* **29** 1062–9

[10] Du B, Mai Y, Chen N and Zhao Y 2023 Doping C60(OH) to regulate the crosslink network and energy band structures of epoxy resin and allow for electronic directional drive in C60(OH)/EP *IEEE Trans. Dielectr. Electr. Insul.* **30** 230–7

[11] Meunier M, Quirke N and Aslanides A 2001 Molecular modeling of electron traps in polymer insulators: chemical defects and impurities *J. Chem. Phys.* **115** 2876–81

[12] Chen L, Huan T D and Ramprasad R 2017 Electronic structure of polyethylene: role of chemical, morphological and

interfacial complexity *Sci. Rep.* **7** 6128

[13] Kubyshkina E, Unge M and Jonsson B L G 2017 Communication: band bending at the interface in polyethylene-MgO nanocomposite dielectric *J. Chem. Phys.* **146** 051101

[14] Takada T, Kikuchi H, Miyake H, Tanaka Y, Yoshida M and Hayase Y 2015 Determination of charge-trapping sites in saturated and aromatic polymers by quantum chemical calculation *IEEE Trans. Dielectr. Electr. Insul.* **22** 1240–9

[15] Zhu M, Li J, Song H, Chen J and Zhang H 2019 Determination of trap energy in polyethylene with different aging status by molecular dynamics and density function theory *IEEE Trans. Dielectr. Electr. Insul.* **26** 1823–30

[16] Yang K, Chen W, Zhao Y, He Y, Chen X, Du B, Yang W, Zhang S and Fu Y 2021 Enhancing dielectric strength of epoxy polymers by constructing interface charge traps *ACS Appl. Mater. Interfaces* **13** 25850–7

[17] Chen J, Chu N, Zhao M, Jin F and Park S J 2020 Synthesis and application of thermal latent initiators of epoxy resins: a review *J. Appl. Polym. Sci.* **137** 49592

[18] Xie Q, Fu K, Liang S, Liu B, Lu L, Yang X, Huang Z and Lü F 2018 Micro-structure and thermomechanical properties of crosslinked epoxy composite modified by nano-SiO2: a molecular dynamics simulation *Polymers* **10** 801

[19] Li J, Zhou F, Min D, Li S and Xia R 2015 The energy distribution of trapped charges in polymers based on isothermal surface potential decay model *IEEE Trans. Dielectr. Electr. Insul.* **22** 1723–32

[20] Zhao Y, Xu Y, Shen H, Du B and Teyssèdre G 2022 Introducing chlorine into epoxy resin to modulate charge trap depth in the material *IEEE Trans. Dielectr. Electr. Insul.* **29** 1666–74